PHYSICS OF FLUIDS **22**, 016101 (2010)

Geometric criterion for RR↔MR transition in hypersonic double-wedge flows

Z. M. Hu,[1,a)] Y. L. Gao,[2] R. S. Myong,[1,b)] H. S. Dou,[3] and B. C. Khoo[3]
[1]*Department of Mechanical and Aerospace Engineering and Research Center for Aircraft Parts Technology, Gyeongsang National University, Jinju 660-701, South Korea*
[2]*Xi'an Research Institute of Hi-Tech, Xi'an, Shaanxi 710025, China*
[3]*Department of Mechanical Engineering, National University of Singapore, Singapore 119260, Singapore*

(Received 18 May 2009; accepted 23 November 2009; published online 8 January 2010)

In a previous research article [Z. M. Hu *et al.*, Phys. Fluids **21**, 011701 (2009)], an overall Mach reflection (oMR) configuration with double inverse Mach reflection patterns was computationally confirmed when a double-wedge geometry interacts with a hypersonic flow. Extended computations are conducted in this paper and compared to analytical solutions based on the classical two- and three-shock theories. A geometric criterion is proposed for the transition between regular reflection and Mach reflection occurring inside the parameter space where a type V interaction of shock wave presents in hypersonic double-wedge flows. An oMR solution is allowed by the geometric criterion, while it is theoretically inadmissible. In the vicinity of symmetric condition, regular to Mach reflection transition can also be triggered prior to the theoretical criterion by disturbance generated by a slight increase in the second wedge angle. © *2010 American Institute of Physics*.
[doi:10.1063/1.3276907]

I. INTRODUCTION

In late 19th century, Ernst Mach found two fundamental shock wave reflection patterns, regular reflection (RR) and Mach reflection (MR). The finding initiated successive study of shock wave interactions. The criteria for the RR↔MR transition of symmetric shock waves, the von Neumann criterion and detachment criterion were introduced by von Neumann (1943).[2] Below the former, a MR wave configuration is theoretically inadmissible, while beyond the latter, a RR configuration is theoretically inadmissible. The two criteria bound a dual-solution domain inside which both RR and MR are theoretically admissible. The state-of-the-art of shock wave interactions and the transition criteria were reviewed by Ben-Dor.[3,4] Hornung *et al.*[5] first hypothesized that hysteresis presents during the RR↔MR transition process. With increasing wedge angle, the RR→MR transition occurs at the detachment condition, while with decreasing wedge angle the MR→RR transition occurs at the von Neumann condition. The hysteresis phenomenon has been proved by experiments when quiet supersonic test facilities became available[6–11] and by computations when high-performance computers were available.[12–18] The research on shock wave interactions is still active in recent times.[1,19–24]

The shock wave interactions have significant impacts on the performance and reliability of a high-speed aircraft. An example is the shock/shock interaction on double-wedge-like geometries in a hypersonic flow which is considered to be a fundamental research problem related to hypersonic flights. Edney[25] used shock polar diagrams and classified the interactions of oblique shock waves and bow shocks on a cylinder. His experimental research proved that abnormally high heating and pressure loads can be induced by shock/shock interactions on the surfaces and that a small variation in the geometry can lead to a major change in overall flow structure. Numerical study was first conducted by Olejniczak *et al.*[26] for shock interactions and their transition among types VI, V, and IV wave patterns over double-wedge-like geometries. It was found that hysteresis and self-induced oscillations in the shock flow pattern can result in extremely high and unsteady loads on the wedge surfaces.[21,27] Thermally nonequilibrium effects on the transition and the oscillation were reported by Hu *et al.*[22] where the thermal properties of the components of air are temperature dependent. Advanced RR→MR transition due to downstream influence has been first reported in a theoretical dual-solution regime.[24] However, the shock interaction phenomena in such a hypersonic background have not been well explained by computations or experiments to the best of our knowledge on related research.

In a previous article, an abnormal MR configuration of asymmetric shock waves was computationally confirmed.[1] Such an overall Mach reflection (oMR) configuration, which is theoretically impossible,[8] consists of two inverse MRs (InMRs) and is denoted as oMR(InMR+InMR) hereafter. The slip layer and the reflection plane form a diverging stream tube in an InMR wave assembly. On the contrary, in a direct MR (DiMR) they form a converging stream tube. Consequently, a DiMR rather than an InMR wave structure in a MR is stable and theoretically admissible because that a converging stream tube is essential to accelerate the subsonic flow downstream the Mach stem to match the overall supersonic flow. The physical mechanism behind the above-

[a)]Author to whom correspondence should be addressed. Electronic mail: bighumin@126.com and tslhz@nus.edu.sg. Present address: Temasek Laboratories, National University of Singapore, 117411, Singapore.
[b)]Electronic mail: myong@gnu.ac.kr.

mentioned oMR(InMR+InMR) wave configuration was found to be the diverging-converging-diverging stream tube generated due to shock wave-slip layer interactions following the shock wave interaction structure. The nomenclature for the wave structures follows the previous work of Li *et al.*[8]

In the present work, extended computations are conducted for a more complete understanding of the transition phenomenon of type V shock interactions,[25] along with theoretical analysis based on the classical two- and three-shock theories. A geometric criterion for RR↔MR transition is then proposed and discussed in detail. It is shown that this proposed criterion, instead of the detachment and von Neumann criteria, governs the wave pattern transition of type V shock wave interactions in hypersonic double-wedge flows.

II. THEORETICAL ANALYSIS

Over a double-wedge geometry, as shown in Fig. 1, a type V interaction[25,26] (see Fig. 2) consists of subsonic and supersonic flow regions. In the wave configuration, the first wedge generates an impinging shock wave LSW1 and the second wedge generates a curved bow shock wave BSW. In the decelerated flow region post shock wave LSW1, an oblique shock wave LSW2 emanates from the wedge corner. Different shock wave patterns possibly occurring in a type V shock interaction are shown in Fig. 1, and the detailed labels can be found in Fig. 2. It should be noted that although the wave structures look similar with those given in the previous work,[22,24] one of the differences is that the whole solution domain instead of the dual-solution domain is of interest in the present study. The flow features the interaction between shock waves of opposite families, SW3 and LSW2. Here, SW3 is a shock wave emanating from the triple-point UTP. As the second wedge angle θ_2 increases, the triple point WTP moves toward the regular interaction point IP, and finally triggers a RR→MR transition at a critical angle $\theta_{2\mathrm{cr}}$.[24] Figures 2(a) and 2(b) show the fundamental flow features for shock interactions of SW3 and LSW2 in which an overall RR (oRR) and an oMR, respectively, emerge. Six- and seven-shock patterns[22,27] were used to distinguish the above two different wave configurations. However, such a taxonomy is incomplete. If SW5 reflects from the second wedge surface in an MR type, as shown in Figs. 2(a) and 2(b), the front of the wave configurations will be composed of eight and nine shock waves, respectively. In the present work, only type V interaction is considered among the possible types of solutions. The details for the type VI interaction in which all flows are supersonic and type IV interaction in which LSW2 detaches from the wedge corner can be referred to the work of Olejniczak *et al.*[26]

Pressure-deflection polar diagrams for shock interaction are applied for the theoretical analysis. Briefly, the shock polar represents the locus of all flow states that can be obtained by passing through a shock wave of a given flow Mach number. The entire region behind a planar shock wave is then represented by a single point on a $p-\theta$ diagram. The flow deflection angle θ and the pressure ratio ξ across an

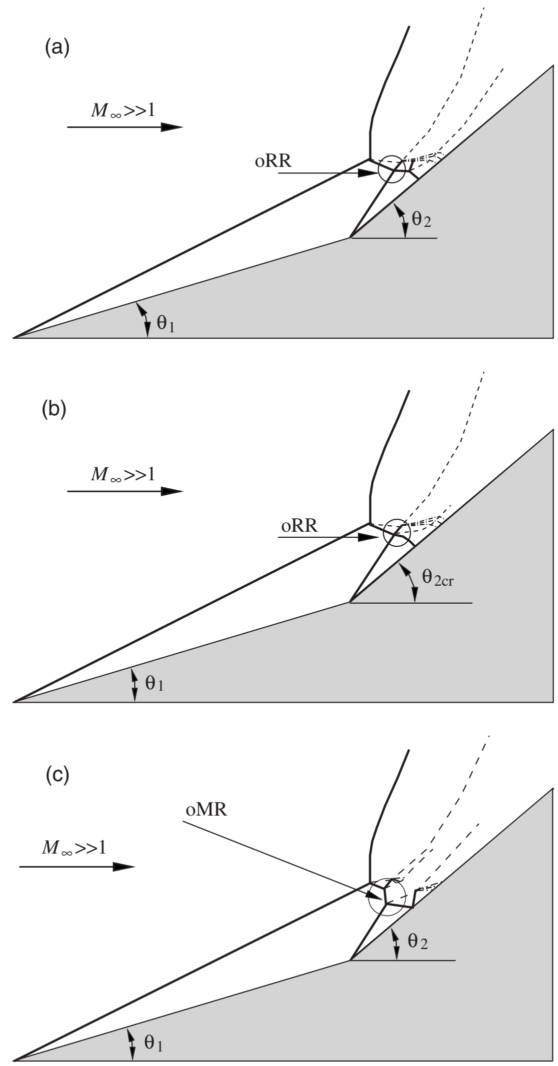

FIG. 1. Fundamental wave configurations of type V shock wave interactions.

oblique shock wave can be, respectively, related to the Mach number M ahead of the shock wave and the shock angle ϕ as follows:

$$\theta = \theta(\gamma, M, \phi) = \arctan\left\{\frac{2\cot\phi(M^2\sin^2\phi - 1)}{M^2(\cos 2\phi + \gamma) + 2}\right\}, \quad (1)$$

$$\xi = \xi(\gamma, M, \phi) = 1 + \frac{2\gamma}{\gamma+1}(M^2\sin^2\phi - 1). \quad (2)$$

Here, ϕ denotes the shock angle, and $\arcsin(1/M) \leq \phi \leq \pi/2$. With above equations, the pressure jump across a shock wave can be plotted against the flow deflection angle.

According to the location of the intersection of R_3-polar with R_1-polar, the MR wave configuration of SW3 can be subclassified into three categories. Figure 3 shows three solution possibilities: DiMR, stationary MR (StMR), and InMR. Here, StMR at the critical wedge angle $\theta_1^{\mathrm{St}\text{-}3}$ is an intermediate case where the slipstream parallels the reflecting plane. In other words, the gas flows of region (1), (4), and (4′) in Fig. 3(b) are in the same direction. The definitions of DiMR and InMR were given in Sec. I. An InMR was

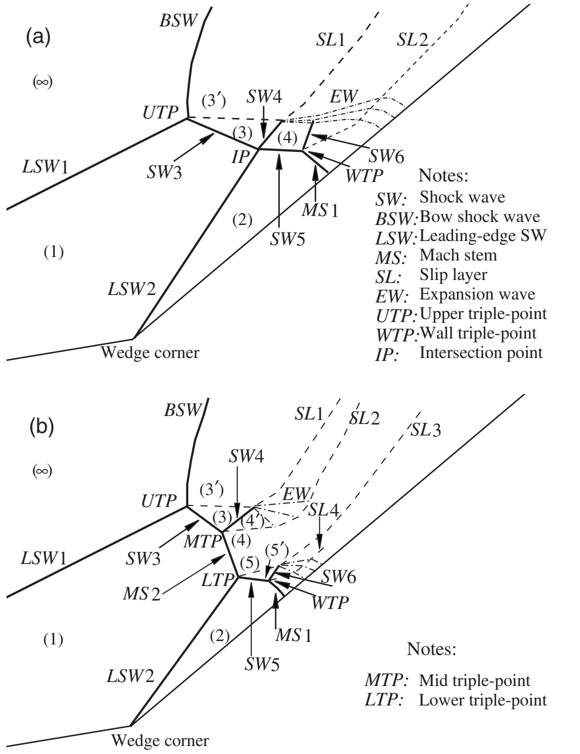

FIG. 2. Fundamental wave configurations of type V shock wave interactions.

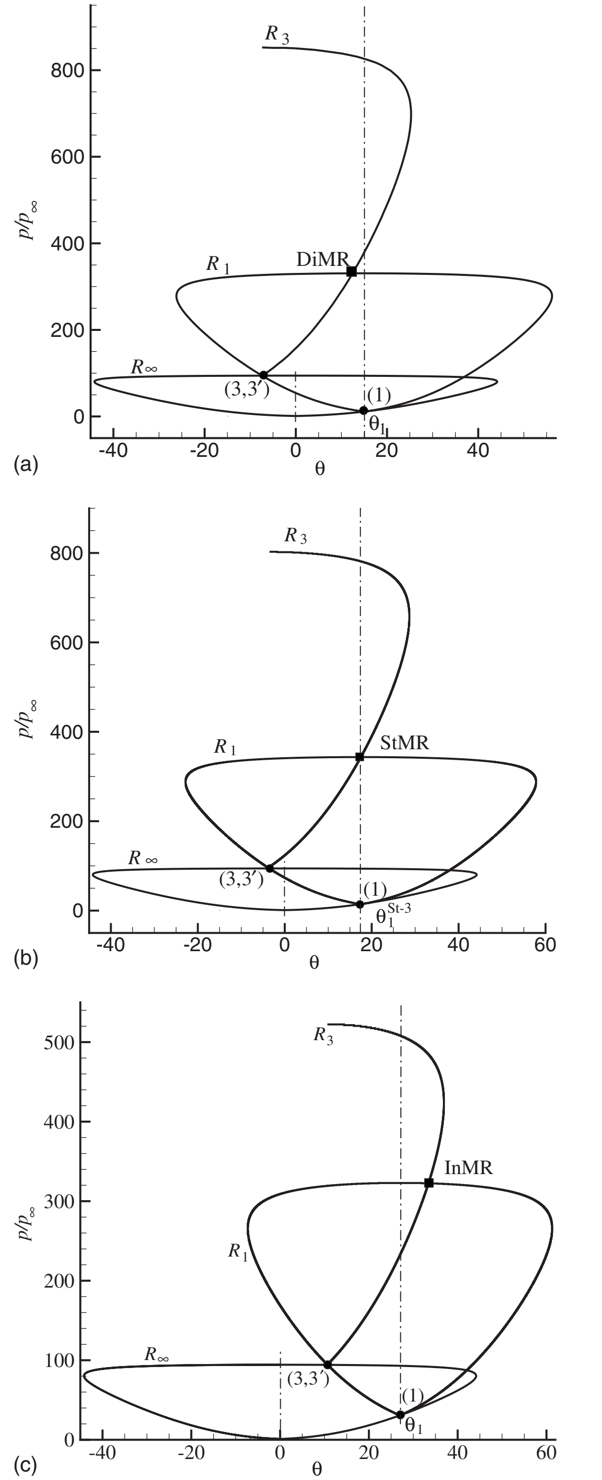

FIG. 3. General pressure-deflection polar combinations illustrating theoretical solutions of three types of MR for shock wave SW3: a DiMR, a StMR, and an InMR, $M_\infty=9$, $\gamma=1.4$.

differently denoted as a wave pattern of a degenerated cross node by Henderson and Menikoff.[28] Such a wave configuration is unstable until appropriate boundary conditions imposed from downstream flowfield. It was reported that an converging-diverging stream tube is essential to bridge the subsonic flow following the Mach stem of an InMR to the global supersonic flow.[1,8] Here, the nomenclature follows the work of Li *et al.*[8]

If $\theta_1<\theta_1^{\text{St-3}}$, the point of intersection between R_3 and R_1 locates along the left-hand branch of R_1-polar. For a given θ_1, three criteria, as shown in Fig. 4(a) divides the theoretical solution of the interaction between LSW2 and SW3 into four solution domains. R_2^D, R_2^{St}, and R_2^{vN}, respectively, denote the loci for LSW2 corresponding to the detachment criterion (θ_2^D), stationary criterion (θ_2^{St}), and von Neumann criterion (θ_2^{vN}).[8] Here, $\theta_2^D>\theta_2^{\text{St}}>\theta_2^{\text{vN}}$. On the contrary, the point of intersection between R_3 and R_1 locates along the right-hand branch of R_1-polar if $\theta_1>\theta_1^{\text{St-3}}$. The relevant criteria for this case are shown in Fig. 4(b) where $\theta_2^D>\theta_2^{\text{vN}}>\theta_2^{\text{St}}$.

For the shock wave interaction between LSW2 and SW3, it is well known that only MR is theoretically possible beyond the detachment criterion θ_2^D, while only RR is theoretically admissible below the von Neumann criterion θ_2^{vN}. Both RR and MR are theoretically possible inside the parameter domain $(\theta_2^{\text{vN}},\theta_2^D)$, which is referred to as the dual-solution domain. The series of critical wedge angles which includes θ_2^{vN}, θ_2^D, θ_2^{St}, and $\theta_1^{\text{St-3}}$ is combined in the $(\Delta\theta-\theta_1)$ parameter space, as given by Fig. 4(c) for hypersonic double-wedge flows with $M_\infty=9$, $\gamma=1.4$. Here, $\Delta\theta=\theta_2-\theta_1$. The whole space can be subdivided into eight sections by the curves corresponding to the aforementioned criteria.

Figures 5(a)–5(d) illustrate four shock polar combinations for a fixed θ_1 and $\theta_1<\theta_1^{\text{St-3}}$. Here, the shock polars R_∞, R_1, and R_3 are all identical, while the polar R_2 changes with θ_2. Note that the intersection point of R_1 and R_3 indicates a DiMR, as shown in Figs. 5(a)–5(d). These four kinds of shock interaction patterns between LSW2 and SW3, along with the three critical conditions illustrated in Fig. 4(a), com-

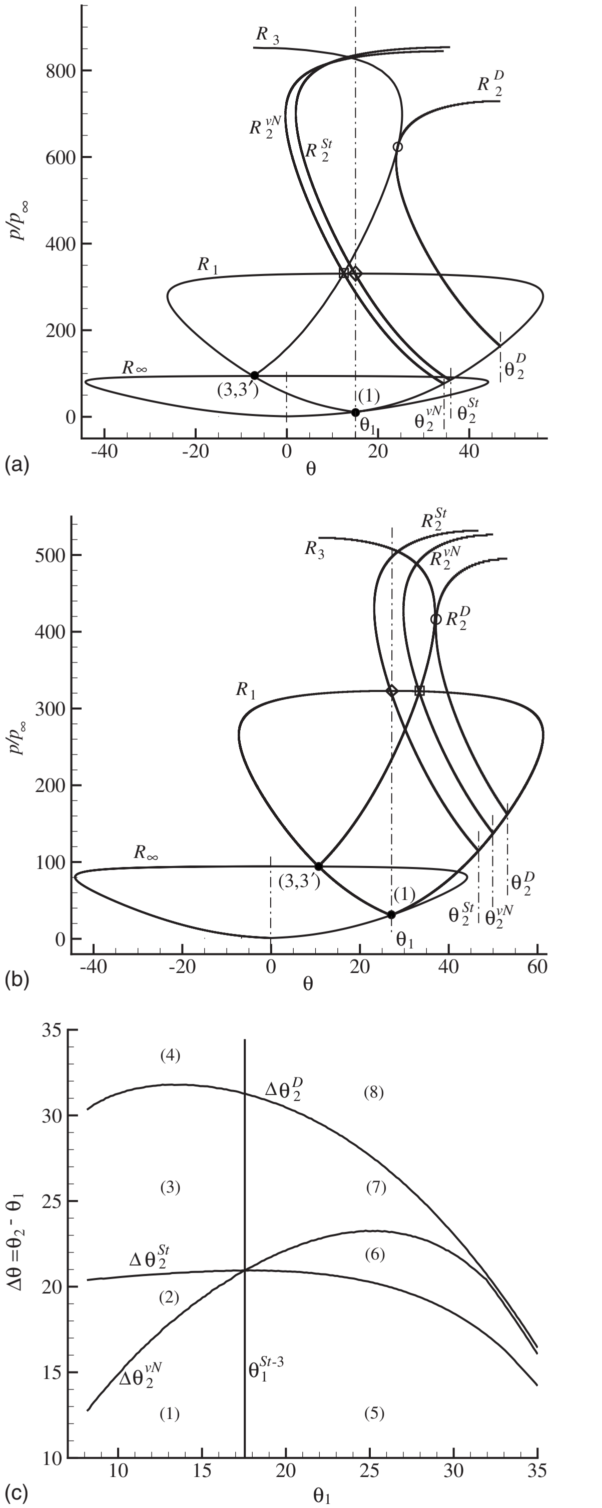

FIG. 4. Critical conditions of θ_2: (a) $\theta_1 < \theta_1^{\mathrm{St\text{-}3}}$, (b) $\theta_1 > \theta_1^{\mathrm{St\text{-}3}}$ as θ_1 is fixed, and (c) on $\Delta\theta - \theta_1$ space, $M_\infty = 9$, $\gamma = 1.4$ (□: von Neumann condition, ◇: StMR condition, and ○: detachment condition).

pose the theoretical solution system consisting of seven categories of wave configurations.

At a low wedge angle $\theta_2 < \theta_2^{\mathrm{vN}}$, the intersection of R_2 and R_3 polars locates inside R_1 polar, which exclusively results in the theoretical solution of an oRR between LSW2 and SW3, as shown in Figs. 2(a) and 5(a). This oRR wave configuration consists of two supersonic RRs (RRsup, labeled by "○"). Because both the slip layers emanating from the triple-point MTP and LTP, as shown in Fig. 2(b) form a diverging stream tube, the MR solution which is an oMR(DiMR+InMR) labeled by "□" in Fig. 5(a) is theoretically impossible. Neither is the subsonic RR (RRsub) labeled by "△." Therefore, the solution domain (1) shown in Fig. 4(c) theoretically allows an oRR wave configuration exclusively.

As a increased wedge angle $\theta_2^{\mathrm{vN}} < \theta_2 < \theta_2^{\mathrm{St}}$, the shock polar combination is shown in Fig. 5(b). The intersection point of R_2 and R_3 locates outside R_1 polar. The MR, an oMR(DiMR+InMR), becomes theoretically admissible because of the converging stream tube assembled between its both slip layers. The RRsup is also a theoretical solution, while the RRsub solution is still theoretically impossible until special boundary conditions is imposed downstream of the interaction point. When $\theta_2^{\mathrm{St}} < \theta_2 < \theta_2^{D}$, both oMR(DiMR+DiMR) and RRsup are theoretical solutions, as shown by Fig. 5(c). It is clear that only MR can occur if $\theta_2^{D} < \theta_2$ as can be seen in Fig. 5(d). Therefore, dual solutions are permitted in the solution domains (2) and (3) shown in Fig. 4(c), while only oMR is allowed in domain (4).

It should be noted clearly that the above analysis is only based on the theoretical relationship of R_2 and R_3 polars. In fact, at the wedge angles of θ_2 shown in Figs. 5(a) and 5(b), the overall shock interaction pattern should be type VI instead of type V. The criterion for type V↔VI transition, $\theta_2^{\mathrm{V}\leftrightarrow\mathrm{VI}}$, is less than the maximum deflection angle of the freestream flow. Type V↔VI transition is not considered in the present study and can be referred to a previous numerical study.[26]

Analogously, Figs. 6(a)–6(d) illustrate four shock polar combinations for a fixed θ_1 and $\theta_1 > \theta_1^{\mathrm{St\text{-}3}}$. Neither of the wave configurations, oMR(InMR+InMR) and oMR(InMR+DiMR), respectively, given in (a) and (b), is theoretically admissible. In general, single solution either of an oRR or of an oMR wave configuration is theoretically reasonable in domains (5), (6), and (8), as shown in Fig. 4(c).

III. COMPUTATIONS ON RR↔MR TRANSITION

As stated by Henderson and Menikoff,[28] the local downstream boundary conditions can affect the solution due to the fact that the wave pattern, in steady state, must be compatible with the global flow. In this section, solutions which are different from the theoretical solutions were explained by computations. The flow condition downstream of the interaction structure varies with the set of angle in a double-wedge geometry. The flow domain of the present interest is shown in Fig. 7 for the inviscid interaction of hypersonic flows and double-wedge geometries. The shock wave interaction phenomena depend on the relevant parameters which are, under the inviscid flow hypothesis, the freestream Mach number M_∞, the ratio of the specific heats γ, the wedge length ratio L_2/L_1, and the wedge angles θ_1 and θ_2. The geometric dimensions are normalized by the first wedge length, L_1. The computational domain surrounded by the dashed-dotted lines, as shown in Fig. 7 is used for computa-

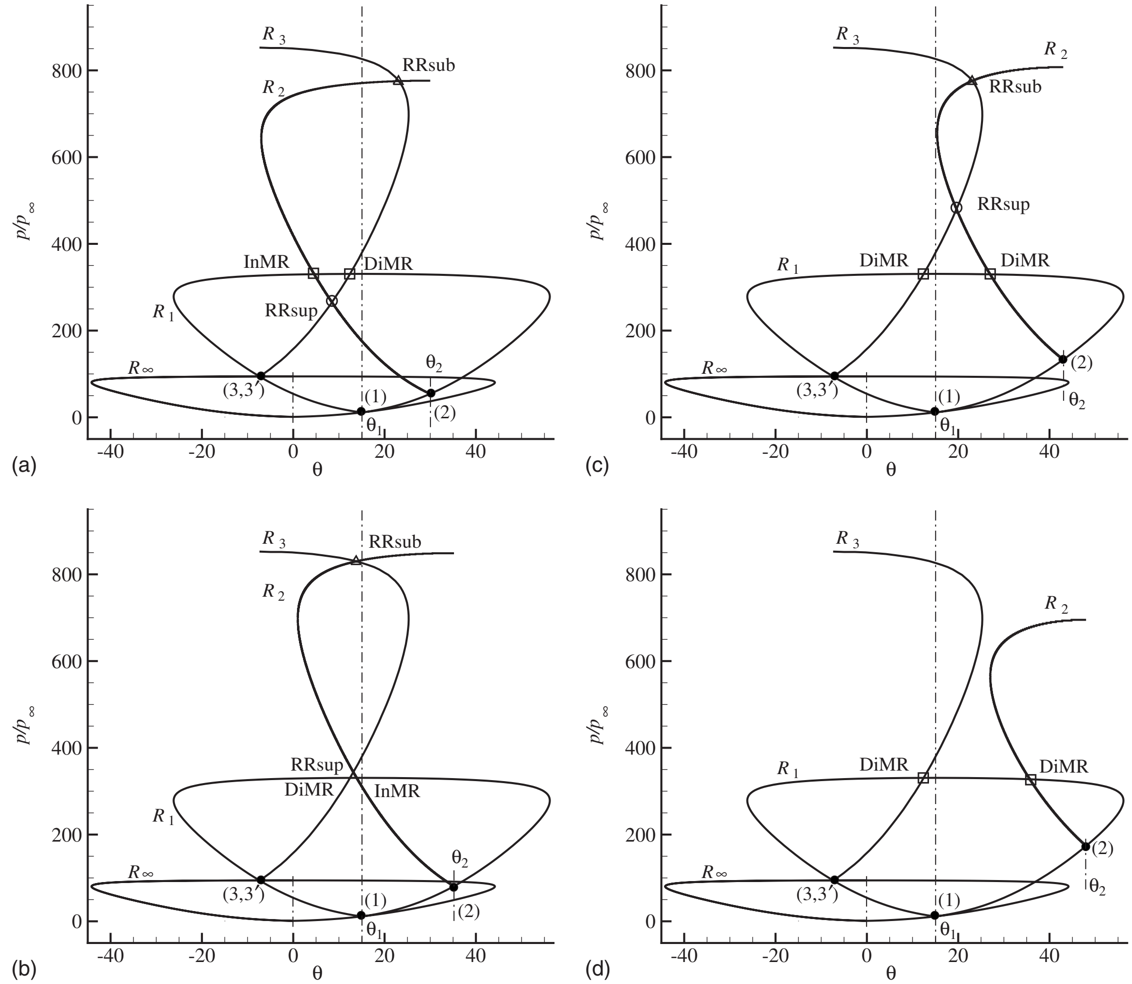

FIG. 5. Different solutions as θ_2 changes, while θ_1 is fixed and $\theta_1 < \theta_1^{\text{St-3}}$, [(a)–(d)] sequentially corresponding to solution domains (1)–(4) shown in Fig. 4(c) (□: MR solution, ○: supersonic RR solution, and △: subsonic RR solution).

tional cheapness. Here, the vertical distance of the first leading shock wave to the wedge corner can be analytically defined as

$$\frac{H}{L_1} = \frac{\sin(\phi_1 - \theta_1)\cos(\phi_1 - \theta_1)}{\cos(\theta_2 - \phi_1)}, \tag{3}$$

where ϕ_1 is the shock angle over the first wedge. In addition, the ratio L_2/L_1 is set to be 0.6 cos θ_2 unless otherwise statement. It should be noted that such a selected domain cannot be used for computations with relative large θ_2 where the upper triple-point, UTP, of the interaction structure may go beyond the left boundary.

It should be noted that thermal and chemical nonequilibrium will be excited under the hypersonic flow mechanism. This brings much more complexity and computational cost to the numerical simulations. For simplicity and conciseness, the flow medium is simplified as a perfect gas with $\gamma=1.4$. The nonequilibrium and dissipative effects are out of the scope of the present computational study. For numerical algorithms in the present study, Euler equations are spatially discretized using the second-order dispersion controlled dissipative (DCD) scheme.[29,30] The principle of DCD is to suppress nonphysical oscillation across strong discontinuities by making use of the intrinsic dispersion characteristics of the modified equations instead of adding artificial viscosity. A third-order Runge–Kutta scheme is used for temporal integration. Uniform supersonic flows with a given Mach number, M_∞ and M_1, are imposed on the left boundary, while a supersonic outflow condition is set on the right boundary. Upper boundary is treated as nonreflecting interfaces, while a slip condition is imposed on the wedge surface.

Several computations for a hypersonic flow with $M_\infty=9$ are shown in Figs. 8(a)–8(d) for different pairs of θ_1 and θ_2 in the vicinity of RR↔MR transitional conditions. In the first two cases, θ_1 is less than $\theta_1^{\text{St-3}}$ and the related theoretical analysis are shown in Figs. 4(a) and 5. The rest cases are all for $\theta_1 > \theta_1^{\text{St-3}}$ and the corresponding theoretical analysis can be found in Figs. 4(b) and 6.

Figures 8(a1)–8(a3) are for the interaction of a $M_\infty=9$ hypersonic flow with a double-wedge-like geometry where $\theta_1=10°$. With a slight increase in θ_2 from 40.2° to 40.5°, the interaction of LSW2 and SW3 undergoes RR→MR transition prior to the corresponding detachment criteria, $\theta_2^D=41.3°$. It was ever reported that the transition can be advanced by the collision between WTP and IP.[1,24] Here, LSW2 and SW3 denote the shock waves emanating from the wedge corner and the upper triple point UTP, respectively. The detailed explanation about the wave structure can be

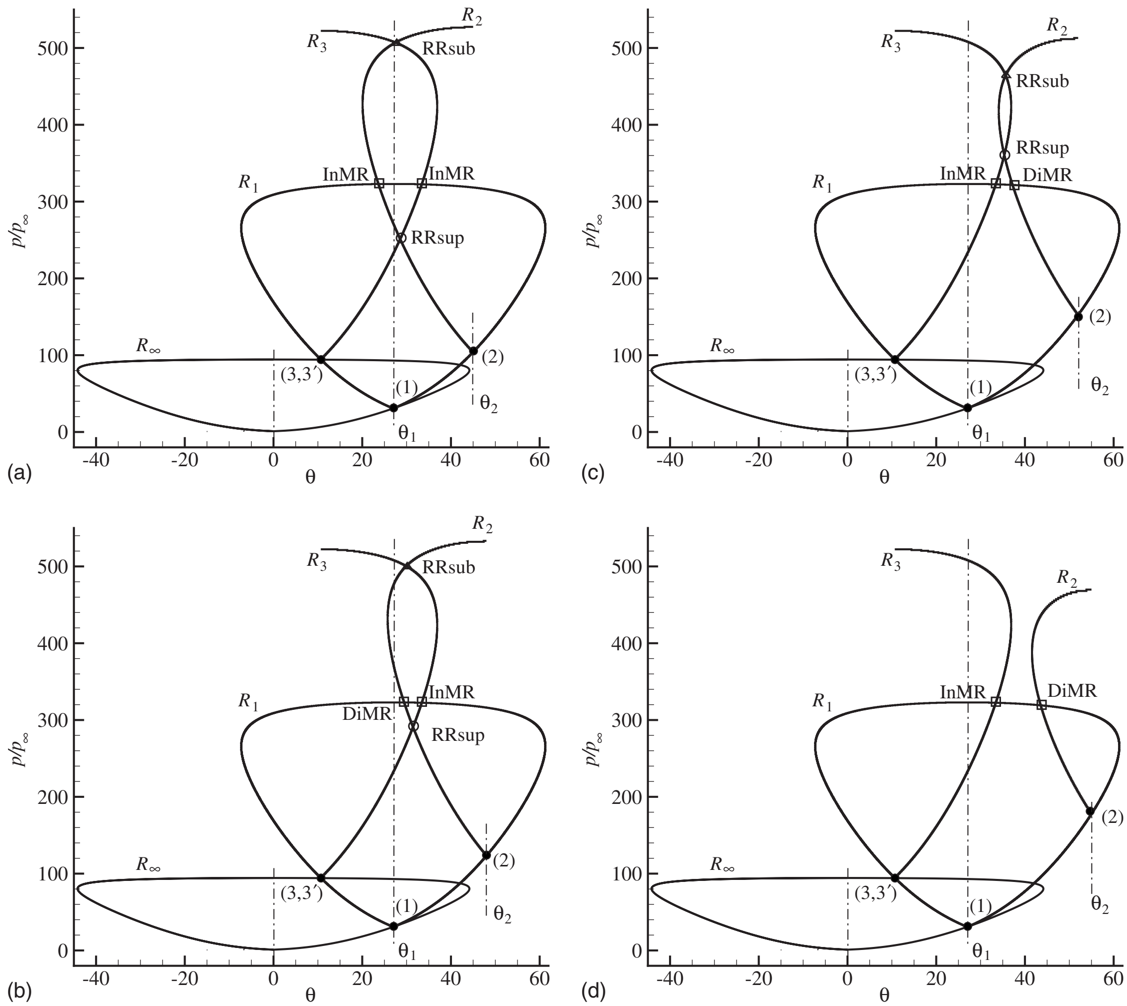

FIG. 6. Different solutions as θ_2 changes, while θ_1 is fixed and $\theta_1 > \theta_1^{\text{St-3}}$, [(a)–(d)] sequentially corresponding to solution domains (5)–(8) shown in Fig. 4(c) (□: MR solution, ○: supersonic RR solution, and △: subsonic RR solution).

found from Fig. 2. Such a mechanism for the advanced RR→MR transition is obvious for the cases shown in Figs. 8(b)–8(d). However, the shock wave SW5 reflects over the wedge surface as a RR in Fig. 8(a1). Therefore, the advanced transition mechanism must be different. It was found that RR→MR transition is relatively easy to be triggered by flow disturbance in the vicinity of the symmetric reflection condition compared with an asymmetric reflection.[24] Figure 9 shows the shock polar combination for the shock interaction over a double-wedge geometry with $\theta_1=10°$, $\theta_2=40.2°$. Here, both of the R_2 and R_3 polars are close to the symmetric line of R_1 polar. Moreover, the RRsup solution labeled by symbol "○" approaches to the sonic point, which is labeled by "▽," of R_2 polar. The specified conditions[24] are satisfied in this case and the RR→MR transition occurs due to the numerical disturbance generated as θ_2 slightly increases. Hereafter, this mechanism for advanced transition is referred to as a disturbance-induced transition (DIT). It should be noted that the maximum pressure load on the second wedge surface increases from $271p_\infty$ to $329p_\infty$ during the transition mentioned above. Significant change of force and heating loads when shock wave pattern varies among types VI, V, and IV interactions has been exposed by previous research.[21,25,26] Here, both wave patterns shown in Figs. 8(a1)–8(a3) are type V interactions according to Edney's classification.[28]

The transition for $\theta_1=15°$ occurring between $\theta_2=41.65°$ and 42.2° is accompanied by an oscillation process of the wave pattern, as shown by Figs. 8(b1) and 8(b2). Figure 8(b2) shows a transient wave pattern featuring an oMR. The unsteady solution results in an oscillating load at a

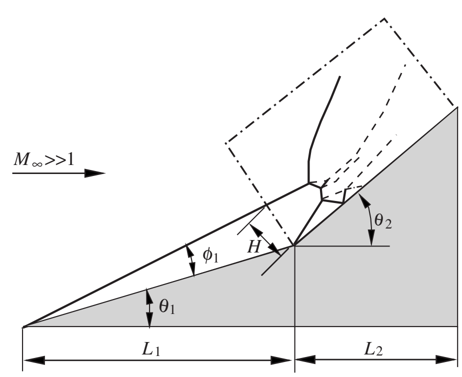

FIG. 7. Flow geometry and the simplified computational domain.

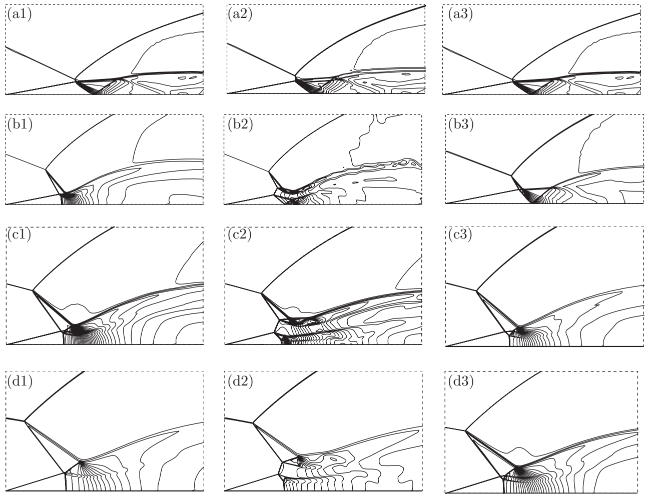

FIG. 8. Computed wave configurations: $\theta_1=10°$, (a1) $\theta_2=40.2°$, (a2) $\theta_2=40.2°\rightarrow40.5°$, (a3) $\theta_2=40.5°\rightarrow40.2°$; $\theta_1=15°$, (b1) $\theta_2=41.65°$, (b2) $\theta_2=42.0°\rightarrow42.2°$, (b3) $\theta_2=41.3°\rightarrow41.1°$; $\theta_1=22.5°$, (c1) $\theta_2=44.2°$, (c2) $\theta_2=44.2°\rightarrow44.4°$, (c3) $\theta_2=44.0°\rightarrow43.8°$; $\theta_1=27°$, (d1) $\theta_2=45.2°$, (d2) $\theta_2=45.2\rightarrow45.4°$, and (d3) $\theta_2=45.2°\rightarrow45.0°$ ($M_\infty=9$, $\gamma=1.4$, grid 651×551).

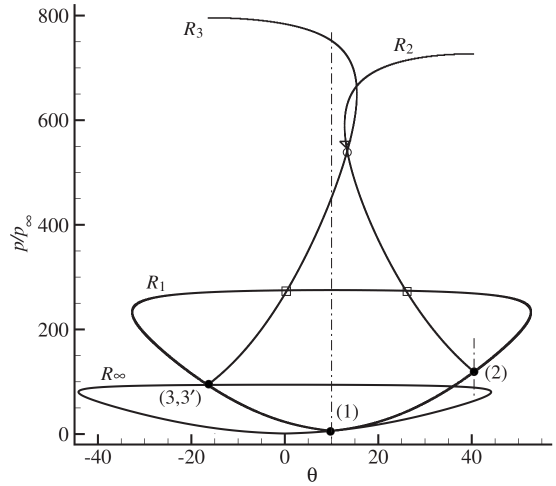

FIG. 9. Shock polar combination for $\theta_1=10°$, $\theta_2=40.2°$ showing a shock interaction in the vicinity of symmetric reflection condition (∇: sonic point).

high frequency over the wedge surface which can cause vital damages to the high-speed vehicles.[21,27] However, the oscillation phenomenon seems to be dependent on the numerical techniques and grid resolution. Wave configurations of oMR and oRR can alternate during an oscillation period in a previous computational study[27] where a W-modification of Godnuv's scheme and relatively coarse mesh were used. In the present study, the applied shock capturing scheme is DCD[29,30] scheme. In a computation using a coarse grid, computed wave configuration can switch between oRR and oMR solutions during an oscillation period, which is similar with findings of the above-mentioned work. The unsteady peak value of pressure along the wedge surface varies between $750p_\infty$ and $1130p_\infty$ within an oscillating period. On the contrary, the oscillating wave configuration maintains an oMR type when mesh of high density is used. The maximum surface pressure, $960p_\infty$, is less than the former. It is also interesting to note that oscillation phenomenon accompanying the RR→MR transition can only be found for $\theta_1=15°$ in the present series of computation. Inside the transitional domain $\theta_2=(40.2°,40.5°)$ for $\theta_1=10°$, the computed wave patterns are all steady. Most interestingly, the wave pattern starts to oscillate at a larger wedge angle $\theta_2=43°$. However, the solution should be theoretically unique and well defined as an oMR configuration because $\theta_2=43°>\theta_2^D$ for case of $\theta_1=10°$. This suggests that the mechanism behind the oscillation phenomenon having nothing to do with the RR→MR transition.

As shown in Figs. 8(c) and 8(d), the critical values of θ_2 for RR→MR transition are amid (44.2°,44.4°) and (45.2°,45.4°) for 22.5° and 27°, respectively. From these cases it is clear that the shock wave SW5 reflects from the second wedge surface as an MR before and after RR→MR transition. Therefore, the maximum surface pressure does not change significantly during the transition process, which is around the normal shock pressure corresponding to R_2 polar. The mechanism for the advanced RR→MR transition for these cases is the collision between the triple point WTP and the intersection point IP as mentioned above. Figure 10(a) shows the geometric parameters, while the RR→MR transition occurs when $h_1(\gamma,M_\infty,\theta_1,\theta_2,L_2/L_1)=h_2(\gamma,M_\infty,\theta_1,\theta_2,L_2/L_1)$. Hereafter, it is referred to as a geometric transition criterion (GTC) of RR→MR in hypersonic double-wedge flows.

The GTC and the DIT (only for the case when $M_\infty=9$ and $\theta_1=10°$) are combined in Fig. 10(b) on the $(\Delta\theta,\theta_1)$ parameter space. Here, symbol "○" denotes computed RR→MR transition point for $M_\infty=9$, while symbol "□" is for the $M_\infty=12$ hypersonic double-wedge flow. The corresponding theoretical criteria as illustrated in Sec. II, $\theta_1^{\text{St-3}}$, θ_2^{vN}, θ_2^{St}, and θ_2^D, are additionally plotted by solid lines for $M_\infty=9$ and dashed lines for $M_\infty=12$ for direct comparison. The oMR solution for the interaction of LSW2 and SW3 when $\theta_1=22.5°$, $\theta_2=44.4°$, and $M_\infty=9$ locates inside the solution domain (6), as labeled in Fig. 4(c), and the corresponding shock polar combination is shown by Fig. 6(b). This suggests a theoretical solution of an oMR(InMR+DiMR) in which the slip layers form a diverging stream tube. Moreover, the computed solution for $\theta_1=27°$, $\theta_2=45.4°$, and $M_\infty=9$ corresponds to an oMR(InMR+InMR) wave configuration according to theoretical analysis, as shown in Fig. 6(a). This type of wave configuration should be theoretically impossible[8] because that the diverging stream tube cannot match the local subsonic flow downstream the Mach stem (i.e., MS2, see Fig. 2) to the global supersonic flow. Therefore, additional boundary conditions should be imposed downstream of the interaction to stabilize such a theoretically unstable oMR(InMR+InMR) wave pattern. In Figs. 8(c2) and 8(d2), the reflected shock wave SW6 impinges on the slip layer SL3 and re-reflected as a series of expansion waves. The impingement and sequential interactions of the expansion waves make SL3 turn upwards. In consequence, SL2 and SL3 assemble a converging stream tube serving as the physical mechanism leading to a steady wave pattern in an oMR(InMR+DiMR) or an oMR(InMR

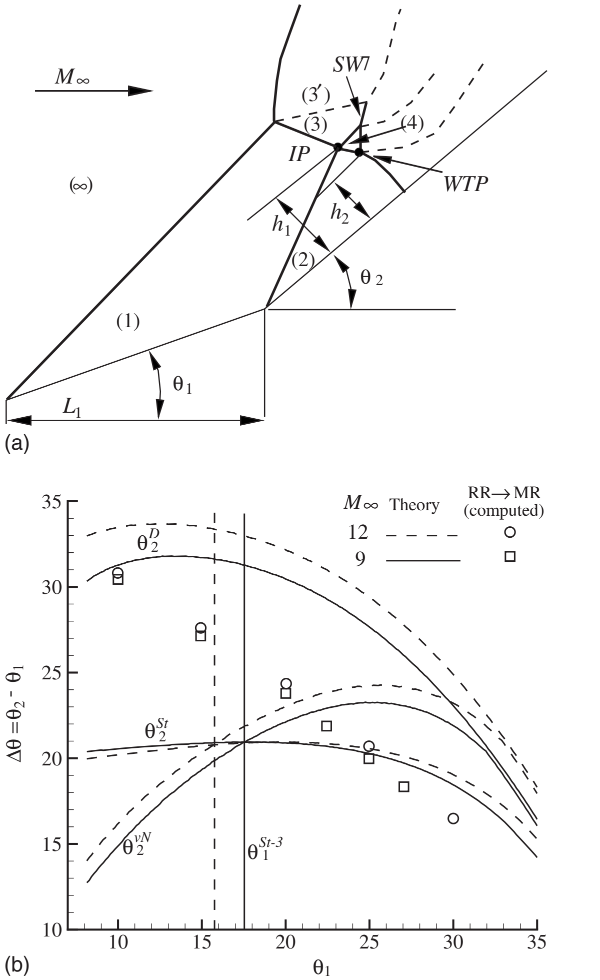

FIG. 10. (a) Geometric parameters and (b) computed geometric criterion of RR↔MR transition for $\gamma=1.4$, $M_\infty=9$, and $M_\infty=12$, respectively.

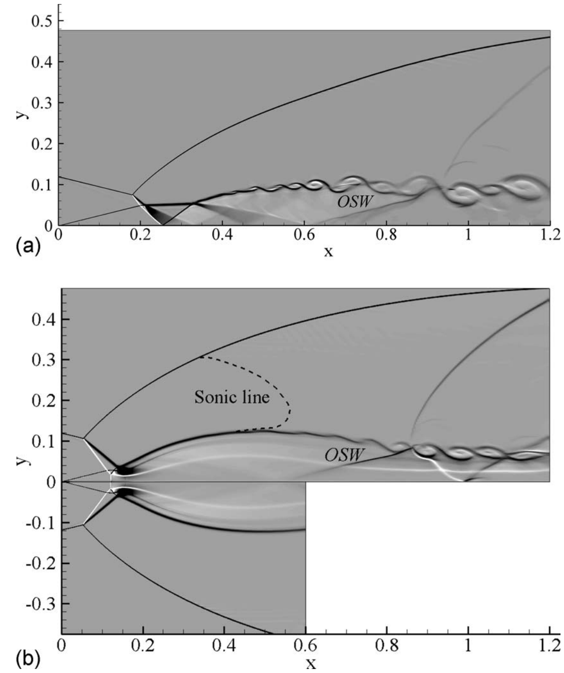

FIG. 11. Numerical schlieren, (a) a transient flow structure during converging process from the computation on a large domain, (b) converged solutions from a larger domain (upper half), and a smaller domain (lower half) ($M_\infty=9$, $\theta_1=22.5°$, $\theta_2=43.0°$)

+InMR) (Ref. 1) wave configuration. The theoretical criteria change significantly for $M_\infty=12$ (dashed lines) compared with those for $M_\infty=9$ (solid lines), as shown in Fig. 10(b). However, the computed RR→MR transition changes slightly with the free-stream flow Mach number implying a weak correlation between the proposed GTC and M_∞.

According the hysteresis phenomenon exposed by previous work,[5–18] the MR→RR transition takes place at the von Neumann condition, θ_2^{vN}, if the wedge angle is gradually decreased from above detachment condition, θ_2^D. As shown in Fig. 8(a3), the MR→RR transition occurs at the same DIT criterion for RR→MR transition at $\theta_1=10°$. For the rest cases (b3)–(d3), however, hysteresis phenomenon occurs during the wave configuration transition. When $\theta_1=15°$, the hysteresis is accompanied by oscillation of oMR wave patterns as θ_2 decreases from 42.2°. MR→RR transition occurs at $\theta_2=41.1°$, which is still far above the corresponding von Neumann condition, $\theta_2^{\mathrm{vN}}=34.4°$, but below the corresponding GTC criterion. For the following cases when $\theta_1=22.5°$ and 27°, slight hysteresis phenomenon is also found but without oscillation of wave patterns.

It should be noted that the numerical RR↔MR transition angles depend on the wedge length ratio L_2/L_1. Figure 11 shows the numerical schlieren obtained on a lager domain of twice length, i.e., $L_2/L_1=1.2\cos\theta_2$ compared with that obtained on the above used domain, as an example. An oblique shock wave, OSW, travels upstream during the converging process, as shown in Fig. 11(a). The moving shock wave/shear layer interaction incurs instability to the shear layer, SL1, which propagates upstream and finally affects the RR→MR transition. The reason to use the computational domain with $L_2/L_1=0.6\cos\theta_2$, corresponding to $x=0.6$, in the computations shown in Fig. 8 and the lower part of Fig. 11(b) is to ensure that (1) the sonic line as plotted by the dashed line in Fig. 11(b) completely stays inside the domain, and (2) the shock wave/shear layer interaction always keeps away from the domain.

IV. CONCLUSIONS

Following a previous study, in this paper, detailed theoretical analysis and computations are conducted for RR↔MR transition of the type V shock wave interaction in hypersonic double-wedge flows. A geometric criterion for RR↔MR transition along with the behind shock wave dynamics is well explained through simulations. As the wedge angle approaching the geometric criterion for a given hypersonic flow, the triple point of a local MR emanating from the second wedge surface collides with the intersection point of an oRR configuration. Such a collision is followed by a transition of the latter to an oMR configuration. In addition, disturbance induced transition is also computationally predicted in the vicinity of symmetric reflection which lies inside the dual-solution domain. Both kinds of transition mechanisms can take place prior to the theoretical detachment criterion based on classical two- and three-shock theories. Furthermore, the RR→MR transition can be advanced at the geometric criterion where an oMR solution is absolutely disallowed by theory. The computations also show that the transition may result in huge changes of pressure and heating loads along the wedge surface if occurring inside the dual-solution domain. On the contrary, the changes are insignificant if the transition occurs below the corresponding von Neumann criterion. A theoretical solution for the computationally proposed geometric criterion may be worked out for further generalization in the future.

ACKNOWLEDGMENTS

The authors, Z.M.H. and R.S.M. were supported by Priority Research Centers Program through the National Research Foundation of Korea (NRF) funded by the Ministry of Education, Science and Technology (Grant No. 2009-0094016) when Z.M.H. was with Gyeongsang National University.

[1] Z. M. Hu, C. Wang, Y. Zhang, and R. S. Myong, "Computational confirmation of an abnormal Mach reflection wave configuration," Phys. Fluids **21**, 011702 (2009).

[2] J. von Neumann, "Refraction, interaction and reflection of shock waves," NAVORD Report No. 203-45, 1943.

[3] G. Ben-Dor, *Shock Wave Reflection Phenomena* (Springer, New York, 2007).

[4] G. Ben-Dor, "A state-of-the-knowledge review on pseudo-steady shock-wave reflections and their transition criteria," Shock Waves **15**, 277 (2006).

[5] H. G. Hornung, H. Oertel, and R. J. Sandeman, "Transitions to Mach reflection of shock waves in steady and pseudo-steady flow with and without relaxation," J. Fluid Mech. **90**, 541 (1979).

[6] A. Chpoun, D. Passerel, H. Li, and G. Ben-Dor, "Reconsideration of oblique shock wave reflections in steady flows. Part 1. Experimental investigation," J. Fluid Mech. **301**, 19 (1995).

[7] B. W. Skews, "Aspect ratio effects in wind tunnel studies of shock wave reflection transition," Shock Waves **7**, 373 (1997).

[8] H. Li, A. Chpoun, and G. Ben-Dor, "Analytical and experimental investigations of the reflection of asymmetric shock waves in steady flows," J. Fluid Mech. **390**, 25 (1999).

[9] B. W. Skews, "Three-dimensional effects in wind tunnel studies of shock wave reflection," J. Fluid Mech. **407**, 85 (2000).

[10] M. S. Ivanov, D. Vandromme, V. M. Fomin, A. N. Kudryavtsev, A. Hadjadj, and D. V. Khotyanovsky, "Transition between regular and Mach reflection of shock waves: New numerical and experimental results," Shock Waves **11**, 199 (2001).

[11] N. Sudani, M. Sato, T. Karasawa, J. Noda, A. Tate, and M. Watanabe, "Irregular effects on the transition from regular to Mach reflection of shock waves in wind tunnel flows," J. Fluid Mech. **459**, 167 (2002).

[12] J. Vuillon, D. Zeitoun, and G. Ben-Dor, "Reconsideration of oblique shock wave reflections in steady flows. Part 2. Numerical investigation," J. Fluid Mech. **301**, 37 (1995).

[13] A. Chpoun and G. Ben-Dor, "Numerical confirmation of the hysteresis phenomenon in the regular to the Mach reflection transition in steady flows," Shock Waves **5**, 199 (1995).

[14] M. Ivanov, D. Zeitoun, J. Vuillon, S. Gimelshein, and G. Markelov, "Investigation of the hysteresis phenomena in steady shock reflection using kinetic and continuum methods," Shock Waves **5**, 341 (1996).

[15] L. F. Henderson, W. Y. Crutchfield, and R. J. Virgona, "The effect of heat conductivity and viscosity of argon on shock waves diffracting over rigid ramps," J. Fluid Mech. **331**, 1 (1997).

[16] G. Ben-Dor, T. Elperin, H. Li, and E. I. Vasilev, "The influence of downstream-pressure on the shock wave reflection phenomenon in steady flows," J. Fluid Mech. **386**, 213 (1999).

[17] M. S. Ivanov, G. Ben-Dor, A. N. Kudryavtsev, and D. V. Khotyyanovsky, "The reflection of asymmetric shock waves in steady flows: A numerical investigation," J. Fluid Mech. **469**, 71 (2002).

[18] A. N. Kudryavtsev, D. V. Khotyanovsky, M. S. Ivanov, A. Hadjadj, and D. Vandromme, "Numerical investigation of transition between regular and Mach reflections caused by free-stream disturbances," Shock Waves **12**, 157 (2002).

[19] C. A. Mouton and H. G. Hornung, "Mach stem height and growth rate predictions," AIAA J. **45**, 1977 (2007).

[20] C. A. Mouton, "Transition between regular reflection and Mach reflection in the dual-solution domain," Ph.D. thesis, California Institute of Technology, 2007.

[21] G. Ben-Dor, T. Elperin, and E. I. Vasilev, "Shock wave-induced extremely high temporal and spatial oscillating pressure peaks," J. Aerosp. Eng. **222**, 653 (2008).

[22] Z. M. Hu, R. S. Myong, C. Wang, T. H. Cho, and Z. L. Jiang, "Numerical study of the oscillations induced by shock/shock interaction in hypersonic double-wedge flows," Shock Waves **18**, 41 (2008).

[23] Z. M. Hu, M. S. Kim, R. S. Myong, and T. H. Cho, "On the RR→MR transition of asymmetric shock waves in steady flows," Shock Waves **18**, 419 (2008).

[24] Z. M. Hu, R. S. Myong, M. S. Kim, and T. H. Cho, "Downstream flow conditions effects on the RR→MR transition of asymmetric shock waves in steady flows," J. Fluid Mech. **620**, 43 (2009).

[25] B. Edney, "Anomalous heat transfer and pressure distributions on blunt bodies at hypersonic speeds in the presence of an impinging shock," The Aerospace Research Institute of Sweden Report No. 115, 1968.

[26] J. Olejniczak, W. J. Wright, and G. V. Candler, "Numerical study of inviscid shock interactions on double-wedge geometries," J. Fluid Mech. **352**, 1 (1997).

[27] G. Ben-Dor, E. I. Vasilev, T. Elperin, and A. V. Zenovich, "Self-induced oscillations in the shock wave flow pattern formed in a stationary supersonic flow over a double wedge," Phys. Fluids **15**, L85 (2003).

[28] L. F. Henderson and R. Menikoff, "Triple shock entropy theorem and its consequences," J. Fluid Mech. **366**, 179 (1998).

[29] Z. L. Jiang, K. Takayama, and Y. S. Chen, "Dispersion conditions for non-oscillatory shock-capturing schemes and its applications," Comput. Fluid Dyn. J. **2**, 137 (1995).

[30] Z. L. Jiang, "On the dispersion-controlled principles for non-oscillatory shock-capturing schemes," Acta Mech. Sin. **20**, 1 (2004).